Robust Hybrid Beamforming for Multi-user Millimeter Wave Systems with Sub-connected Structure

Zhen Luo(✉), Lang Luo, Xin Zhang, and Hongqing Liu

School of Communication and Information Engineering, Chongqing University of Posts and Telecommunications, Chongqing 404100, China
luozhen@cqupt.edu.cn, {s210131170,s190131221}@stu.cqupt.edu.cn

Abstract. In this paper, we investigate a millimeter wave multi-user system to further improve the spectral efficiency. Millimeter wave channels with correlated estimation errors and sub-connected structures are considered to develop a two-stage hybrid beamforming scheme. In the first stage, the analog parts of beamformers are designed to maximize RF-to-RF channel gains. In the second stage, the digital parts of the beamformers are optimized by utilizing the equivalence between the maximization of mutual information and the minimization of weighted minimum mean square error. The numerical results show that the proposed scheme has superior performance over other existing designs.

Keywords: millimeter wave · hybrid beamforming · multi-user · estimation errors · sub-connected

1 Introduction

With the increasing congestion of sub-6GHz, millimeter wave (mmWave) band receives wide research interests as the unexploited band for the fifth-generation mobile communication. The severe path loss caused by short wavelength is the main obstacle to the utilization of mmWave [1]. Fortunately, short wavelength also enables small devices to package a large number of antennas. Thus, the current enabling technology is to develop beamforming schemes which steers the transmitting/receiving beams in a certain direction to combat the path loss. However, for conventional multiple-input multiple-output (MIMO) systems with fully digital beamforming, each transmitting or receiving antenna need to assign one radio frequency (RF) chain. Applying such structure to mmWave systems with large antenna arrays results in extremely high power consumption and hardware complexity [2], which is unaffordable in practice. So hybrid beamforming, which consists of analog part with only phase shifters and digital part with small number of RF chains, is widely adopted in mmWave beamforming designs due to the balance of cost, complexity, and system performance.

F. Gao et al. (Eds.): ChinaCom 2022, LNICST 500, pp. 109–121, 2023.
https://doi.org/10.1007/978-3-031-34790-0_9

The hybrid beamforming schemes for multi-user (MU) systems have been studied in literature. In [3], the fully digital beamformer of each user is designed to minimize the total mean square error (MSE) first. Then, the OMP-based algorithm is applied to decompose the fully digital processors into hybrid ones. However, the computational complexity of decomposing a matrix with large antenna arrays is extremely high. To reduce the computational complexity, the two-stage design scheme, which designs analog and digital beamformers successively, is adopted in [4–8]. In [4], the analog beamformers are determined firstly, and the digital beamformers are designed to minimize the sum-MSE. In [5], a joint design method is proposed to avoid the loss of information at each stage. In [6], the analog and digital beamformers are updated iteratively to minimize MSE. In [7], a piecewise successive iterative approximation algorithm is utilized to design analog beamformers, and digital beamformers are designed by piecewise successive approximation to avoid the loss of information. The aforementioned works all adopt fully-connected structures in which each RF chain is connected to all antennas. However, such a structure leads to severe insertion losses and degrades the energy efficiency [9]. Thus, sub-connected structure is adopted in [8]. The analog beamformers are designed to maximize RF-to-RF channel gains, and the digital beamformers are obtained by applying zero-forcing (ZF) strategy to eliminate the inter-user interference.

It is noted that the above works are all based on perfect channel state information (CSI) assumptions. However, CSI imperfectness must be considered in implementations. The estimation errors of angles are considered in [10,11]. In [12], a robust hybrid beamforming scheme is proposed for MU full-duplex systems based on uncorrelated estimation errors. Correlated estimation errors are investigated in [13] for point-to-point mmWave systems, in which the compressed sensing based algorithm applicable for mmWave channels is considered to derive the estimated channel model. To the best of our knowledge, the hybrid beamforming design for MU systems based on correlated estimation errors is still an open problem.

We develop a robust hybrid beamforming scheme with sub-connected structures for MU systems in this paper. Unlike the study in [8], which assumes single data steam users, a more general situation where each user is equipped with multiple RF chains to support multiple data streams is investigated in this paper. The analog parts of beamformers are designed to maximize the gains of RF-to-RF channels. The optimization of digital beamformers is solved iteratively by utilizing the equivalence between the maximization of mutual information and the minimization of weighted minimum mean square error (WMMSE). The main contributions are summarized as follows: 1) A robust hybrid beamforming scheme is proposed for MU mmWave systems based on correlated estimation errors. 2) To improve energy efficiency, the sub-connected structure is adopted in this paper. To the best of our knowledge, this is the first robust design for such system configurations. Performance gains of the proposed design are highlighted by numerical simulations in terms of sum rates and energy efficiencies.

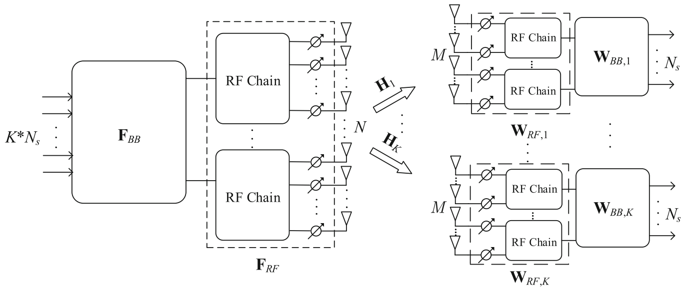

Fig. 1. System model.

Notation: Bold lower case and upper case letters denote vectors and matrices, respectively. $(\cdot)^T$, $(\cdot)^H$, $\mathrm{tr}(\cdot)$, $E(\cdot)$ stand for the matrix transpose, Hermitian transpose, trace and expectation, respectively. $\|\cdot\|_F$ denotes the Frobenius norm. $\mathbf{x}^{(i)}$ is the i-th entry of vector $\mathbf{x}$. $\mathbf{X}(m:n,i)$ denotes the sub-matrix composed of corresponding rows and column of $\mathbf{X}$. $\mathbf{I}_K$ denotes the $K \times K$ identity matrix. $\mathbb{C}^{N\times M}$ is the set of all $N \times M$ complex matrices. $\mathbf{X} \sim \mathcal{CN}(\mathbf{P}, \mathbf{K})$ means that $\mathbf{X}$ is a complex Gaussian random matrix with mean $\mathbf{P}$ and covariance matrix $\mathbf{K}$.

2 System and Channel Model

The downlink of the MU mmWave system with sub-connected structure is illustrated in Fig. 1, where a base station (BS) with N antennas serves K users with M antennas on each user. Hybrid structures are employed at the BS and users. The BS is equipped with KN_{rf} RF chains to support KN_s data streams, and each user is equipped with N_{rf} RF chains to support N_s data streams. The number of RF chains is subject to the constraint $N_s \leq N_{rf} \leq \min\{\frac{N}{K}, M\}$. The signal transmitted at the BS can be expressed as

$$\mathbf{x} = \mathbf{F}_{RF}\mathbf{F}_{BB}\mathbf{s}, \tag{1}$$

where $\mathbf{F}_{RF} \in \mathbb{C}^{N\times KN_{rf}}$ denotes the analog precoder at the BS; $\mathbf{F}_{BB} = [\mathbf{F}_{BB,1}, \cdots, \mathbf{F}_{BB,K}]$ with $\mathbf{F}_{BB,k} \in \mathbb{C}^{KN_{rf}\times N_s}, k \in \{1, 2, \cdots, K\}$ denoting the digital precoder at the BS associated with the k-th user; $\mathbf{s} = [\mathbf{s}_1^T, \cdots, \mathbf{s}_K^T]^T \in \mathbb{C}^{KN_s\times 1}$ is the transmitted signal, with $\mathbf{s}_k \in \mathbb{C}^{N_s\times 1}$ is the signal intended for the k-th user, which satisfies $E(\mathbf{s}\mathbf{s}^H) = I_{KN_s}$. The power constraint at the BS is $\sum_{j=1}^{K} \mathrm{tr}\left(\mathbf{F}_{RF}\mathbf{F}_{BB,j}\mathbf{F}_{BB,j}^H\mathbf{F}_{RF}^H\right) = 1$. The combined signal at the k-th user $\mathbf{y}_k$ can be expressed as

$$\begin{aligned}\mathbf{y}_k = {} & \mathbf{W}_{BB,k}^H\mathbf{W}_{RF,k}^H\mathbf{H}_k\mathbf{F}_{RF}\mathbf{F}_{BB,k}\mathbf{s}_k + \mathbf{W}_{BB,k}^H\mathbf{W}_{RF,k}^H\mathbf{H}_k \\ & \cdot \mathbf{F}_{RF}\sum_{h=1,h\neq k}^{K}\mathbf{F}_{BB,h}\mathbf{s}_h + \mathbf{W}_{BB,k}^H\mathbf{W}_{RF,k}^H\mathbf{n}_k,\end{aligned} \tag{2}$$

where $\mathbf{W}_{BB,k} \in \mathbb{C}^{N_{rf} \times N_s}$ denotes the digital combiner at the k-th user; $\mathbf{W}_{RF,k} \in \mathbb{C}^{M \times N_{rf}}$ is the analog combiner at the k-th user; $\mathbf{H}_k \in \mathbb{C}^{M \times N}$ is the channel matrix from the BS to the k-th user, and $\mathbf{n}_k \sim \mathcal{CN}(\mathbf{0}, \sigma^2_{\mathbf{n}_k}\mathbf{I}_M)$ is the corresponding complex additive white Gaussian noise (AWGN).

Notice that because of the sub-connected structure, analog beamformers are constrained as follows:

$$\mathbf{F}_{RF} = [\mathbf{f}_{rf,1}, \cdots, \mathbf{f}_{rf,KN_{rf}}], \tag{3}$$

$$\mathbf{W}_{RF,k} = [\mathbf{w}_{rf,k,1}, \cdots, \mathbf{w}_{rf,k,N_{rf}}], \tag{4}$$

where $\mathbf{f}_{rf,p} \in \mathbb{C}^{N\times 1}, p \in \{1, \cdots, KN_{rf}\}$ with non-zero elements in $[(p-1)M_s+1]$-th to pM_s-th element, $\mathbf{w}_{rf,k,q} \in \mathbb{C}^{M\times 1}, q \in \{1, \cdots, N_{rf}\}$ with non-zero elements in $[(q-1)M_d+1]$-th to qM_d-th element. $M_s = \frac{N}{KN_{rf}}$ and $M_d = \frac{M}{N_{rf}}$ are the number of antennas connected to each RF chain at the BS and the k-th user, respectively. In this paper, we assume that M_d of each user is the same for simplicity. As the analog beamformers are implemented by phase shifters, none-zero elements in analog beamforming matrices satisfy that $|\mathbf{f}^{(c)}_{rf,p}| = \sqrt{\frac{1}{M_s}}$, $|\mathbf{w}^{(d)}_{rf,q}| = \sqrt{\frac{1}{M_d}}$, for $\forall c, d$.

The mmWave channel with a uniform linear array can be formulated as follows

$$\mathbf{H} = \sqrt{\frac{NM}{N_p}} \sum_{m=1}^{N_p} \alpha_m \mathbf{a}_r(\theta_m)\, \mathbf{a}_t(\phi_m)^H, \tag{5}$$

where N_p is the number of scattering paths; α_m denotes the complex gain of the m-th scattering path; $\mathbf{a}_r$ and $\mathbf{a}_t$ denote the receive and transmit array response vectors with the angle of arrival (AoA) θ_m and the angle of departure (AoD) ϕ_m, respectively. The channel can be rewritten compactly as follows

$$\mathbf{H} = \mathbf{A}_r \mathbf{D} \mathbf{A}_t^H, \tag{6}$$

where $\mathbf{A}_r = [\mathbf{a}_r(\theta_1), \cdots, \mathbf{a}_r(\theta_{N_p})]$ and $\mathbf{A}_t = [\mathbf{a}_t(\phi_1), \cdots, \mathbf{a}_t(\phi_{N_p})]$ are the receive and transmit array response vector sets, respectively. $\mathbf{D}$ is a diagonal matrix, with the m-th diagonal element being $\sqrt{\frac{NM}{N_p}}\alpha_m$. The relationship between the actual channel and the estimated channel can be expressed as [13]

$$\bar{\mathbf{H}} = \mathbf{H} + \mathbf{N}\mathbf{\Phi}, \tag{7}$$

where $\mathbf{\Phi}$ is the estimation processing matrix. $\mathbf{N} \sim \mathcal{CN}(\mathbf{0}, \sigma_e^2\mathbf{I})$ denotes the AWGN during the training period. The channel model in (7) applies to all the channels in the system, we drop the subscripts here for ease of notation. For more details about the correlated channel model, please refer to [13].

Notice that, the estimation algorithms applicable for mmWave channels will result in correlated errors, as described in (7). So the existing robust designs based on uncorrelated channel model in [12] are not applicable now. In the Sect. 4, the numerical results will show the loss of performance due to the mismatch of the channel model.

3 Robust Hybrid Beamforming Designs

In this section, a two-stage scheme is developed to design hybrid beamformers. In the first stage, the analog beamformers are designed to maximize estimated RF-to-RF channel gains. In the second stage, the digital beamformers are optimized by utilizing the equivalence between the maximization of mutual information and the minimization of WMMSE.

3.1 Analog Beamforming Designs

The RF-to-RF estimated channel at the k-th user can be expressed as

$$\hat{\mathbf{H}}_k = \mathbf{W}_{RF,k}^H \bar{\mathbf{H}}_k \mathbf{F}_{RF}. \tag{8}$$

The gain of the i-th eigenmode in the k-th RF-to-RF estimated channel can be express as

$$\left|\mathbf{w}_{rf,k,i}^H \bar{\mathbf{u}}_{k,i} \bar{\mathbf{v}}_{k,i}^H \mathbf{f}_{rf,(k-1)N_{rf}+i}\right|, \tag{9}$$

where $i \in \{1, \cdots, N_{rf}\}$; $\mathbf{u}_{k,i}$ and $\mathbf{v}_{k,i}$ are the i-th columns in left and right singular matrices i.e., $\bar{\mathbf{U}}_k$ and $\bar{\mathbf{V}}_k$, of $\bar{\mathbf{H}}_k$, with ordered singular value decomposition $\bar{\mathbf{H}}_k = \bar{\mathbf{U}}_k \bar{\mathbf{\Lambda}}_k \bar{\mathbf{V}}_k^H$. The analog beamformers are design as follows

$$\begin{aligned} &\mathbf{w}_{rf,k,i}[(i-1)M_d + 1 : iM_d] = \\ &\qquad \sqrt{\frac{1}{M_d}} \cdot \text{phase}\left\{\bar{\mathbf{U}}_k[(i-1)M_d + 1 : iM_d, i]\right\}, \end{aligned} \tag{10}$$

$$\begin{aligned} &\mathbf{f}_{rf,(k-1)N_{rf}+i}[((k-1)N_{rf} + i - 1)M_s + 1 : \\ &\qquad ((k-1)N_{rf} + i)M_s] = \\ &\qquad \sqrt{\frac{1}{M_s}} \cdot \text{phase}\left\{\bar{\mathbf{V}}_k[(i-1)M_s + 1 : iM_s, i]\right\}, \\ &\qquad\qquad k \in \{1, \cdots, K\}. \end{aligned} \tag{11}$$

Proof. $\mathbf{w}_{rf,k,i}$ and $\mathbf{f}_{rf,(k-1)N_{rf}+i}$ can be expressed as

$$\begin{aligned} \mathbf{w}_{rf,k,i} &= \sqrt{\frac{1}{M_d}}[\mathbf{0}_{1\times(i-1)M_d}, e^{j\theta_1^{(k,i)}}, \cdots, e^{j\theta_{M_d}^{(k,i)}}, \\ &\qquad \mathbf{0}_{1\times M-iM_d}]^T, \\ \mathbf{f}_{rf,(k-1)N_{rf}+i} &= \sqrt{\frac{1}{M_s}}[\mathbf{0}_{1\times((k-1)N_{rf}+i-1)M_s}, e^{j\phi_1^{(k,i)}}, \\ &\qquad \cdots, e^{j\phi_{M_s}^{(k,i)}}, \mathbf{0}_{1\times N-((k-1)N_{rf}+i)M_s}]^T. \end{aligned} \tag{12}$$

The polar forms of $\bar{\mathbf{u}}_{k,i}$ and $\bar{\mathbf{v}}_{k,i}$ are $\bar{\mathbf{u}}_{k,i} = [\gamma_1 e^{j\alpha_1^{(k,i)}}, \cdots, \gamma_M e^{j\alpha_M^{(k,i)}}]^T$, $\bar{\mathbf{v}}_{k,i} = [\rho_1 e^{j\beta_1^{(k,i)}}, \cdots, \rho_N e^{j\beta_N^{(k,i)}}]^T$. Then, the gain of the i-th eigenmode in the k-th RF-to-RF estimated channel can be expressed as

$$\begin{aligned}&\left|\mathbf{w}_{rf,k,i}^{H}\bar{\mathbf{u}}_{k,i}\bar{\mathbf{v}}_{k,i}^{H}\mathbf{f}_{rf,(k-1)N_{rf}+i}\right| = \\&\left|\sqrt{\frac{1}{M_d}}\sum_{f=(i-1)M_d+1}^{iM_d}\gamma_f e^{(\theta_f^{(k,i)}-\alpha_f^{(k,i)})}\right| \\&\cdot\left|\sqrt{\frac{1}{M_s}}\sum_{g=((k-1)N_{rf}+i-1)M_s+1}^{((k-1)N_{rf}+i)M_s}\rho_g e^{(\beta_g^{(k,i)}-\phi_g^{(k,i)})}\right|.\end{aligned} \tag{13}$$

According to the Cauchy-Schwartz inequality, we have

$$\begin{aligned}&\left|\sqrt{\frac{1}{M_d}}\sum_{f=(i-1)M_d+1}^{iM_d}\gamma_f e^{(\theta_f^{(k,i)}-\alpha_f^{(k,i)})}\right|^2 \\&\leq \frac{1}{M_d}\sum_{f=(i-1)M_d+1}^{iM_d}|\gamma_f|^2\sum_{f=(i-1)M_d+1}^{iM_d}\left|e^{(\theta_f^{(k,i)}-\alpha_f^{(k,i)})}\right|^2 \\&= \frac{1}{M_d}\sum_{f=(i-1)M_d+1}^{iM_d}|\gamma_f|^2.\end{aligned} \tag{14}$$

The equality holds when $\theta_f^{(k,i)} = \alpha_f^{(k,i)}$, $\forall f$. Similarly, $|\bar{\mathbf{v}}_{k,i}^{H}\mathbf{f}_{rf,(k-1)N_{rf}+i}|$ has the maximum when $\beta_g^{(k,i)} = \phi_g^{(k,i)}$, $\forall g$. So we have the conclusion in (10) and (11).

3.2 Digital Beamforming Designs

After determining the analog beamformers, the problem is reduced to optimization of low-dimensional digital beamformers. After fixing the analog beamformers, the k-th effective channel can be constructed as

$$\tilde{\mathbf{H}} = \hat{\mathbf{H}}_k + \mathbf{\Sigma}_k\mathbf{N}_k\mathbf{\Psi}_k \tag{15}$$

where $\mathbf{\Sigma}_k = \mathbf{W}_{RF,k}^{H}$; $\mathbf{\Psi}_k = \mathbf{\Phi}_k\mathbf{F}_{RF}$. Substituting (15) into (2), the k-th combined signal can be rewritten as

$$\begin{aligned}\mathbf{y}_k = \mathbf{W}_{BB,k}^{H}\tilde{\mathbf{H}}_k\mathbf{F}_{BB,k}\mathbf{s}_k + \mathbf{W}_{BB,k}^{H}\tilde{\mathbf{H}}_k\sum_{h=1,h\neq k}^{K}\mathbf{F}_{BB,h}\mathbf{s}_h \\ + \mathbf{W}_{BB,k}^{H}\tilde{\mathbf{n}}_k,\end{aligned} \tag{16}$$

where $\tilde{\mathbf{n}}_k = \mathbf{W}_{RF,k}^H \mathbf{n}_k$. To simplify the design, the minimum mean square error (MMSE) receiver is adopted, which is given by

$$\mathbf{W}_{BB,k} = \left[\hat{\mathbf{H}}_k \left(\sum_{j=1}^{K} \mathbf{F}_{BB,j} \mathbf{F}_{BB,j}^H \right) \hat{\mathbf{H}}_k^H + \mathbf{Q}_k \right]^{-1} \cdot \hat{\mathbf{H}}_k \mathbf{F}_{BB,k}, \tag{17}$$

where $\mathbf{Q}_k = \sum_{j=1}^{K} \sigma_e^2 \mathrm{tr}\left(\mathbf{\Psi}_k \mathbf{F}_{BB,j} \mathbf{F}_{BB,j}^H \mathbf{\Psi}_k^H \right) \mathbf{\Sigma}_k \mathbf{\Sigma}_k^H + \mathbf{R}_{\tilde{n}_k}$ is obtained by utilizing Lemma 3 in [14]; $\mathbf{R}_{\tilde{n}_k} = E\left(\tilde{\mathbf{n}}_k \tilde{\mathbf{n}}_k^H \right) = \sigma_{\mathbf{n}_k}^2 \mathbf{W}_{RF,k}^H \mathbf{W}_{RF,k}$.

Then, the digital precoder at the BS is designed to maximize the lower bound of average mutual information, which is given by [15]

$$I_{lb}\left(\mathbf{s}_k, \tilde{\mathbf{y}}_k \right) = -\log\det \mathbf{M}_k, \tag{18}$$

where $\tilde{\mathbf{y}}_k$ denotes the received signal before combining at the k-th user; $\mathbf{M}_k$ is the MMSE matrix of the k-th user, which can be formulated as

$$\begin{aligned} \mathbf{M}_k = & \mathbf{W}_{BB,k}^H \left[\hat{\mathbf{H}}_k \sum_{j=1}^{K} \left(\mathbf{F}_{BB,j} \mathbf{F}_{BB,j}^H \right) \hat{\mathbf{H}}_k^H + \mathbf{Q}_k \right] \mathbf{W}_{BB,k} \\ & - \mathbf{W}_{BB,k}^H \hat{\mathbf{H}}_k \mathbf{F}_{BB,k} - \mathbf{F}_{BB,k}^H \hat{\mathbf{H}}_k^H \mathbf{W}_{BB,k} + \mathbf{I}_{N_s}. \end{aligned} \tag{19}$$

The optimization problem can be formulated as

$$\begin{aligned} \max_{\{\mathbf{F}_{BB,j}\}} \ & \sum_{j=1}^{K} I_{lb}\left(\mathbf{s}_j, \tilde{\mathbf{y}}_j \right) \\ \text{s.t.} \ & \sum_{j=1}^{K} \mathrm{tr}\left(\mathbf{F}_{RF} \mathbf{F}_{BB,j} \mathbf{F}_{BB,j}^H \mathbf{F}_{RF}^H \right) = 1. \end{aligned} \tag{20}$$

It is still difficult to directly solve the above problem. Therefore, the equivalence between the maximization of mutual information and the minimization of WMMSE is utilized in this paper. The minimization problem of WMMSE is formulated as follows

$$\begin{aligned} \min_{\{\mathbf{F}_{BB,j}, \mathbf{V}_j\}} \ & \sum_{j=1}^{K} \mathrm{tr}\left(\mathbf{V}_j \mathbf{M}_j \right) \\ \text{s.t.} \ & \sum_{j=1}^{K} \mathrm{tr}\left(\mathbf{F}_{RF} \mathbf{F}_{BB,j} \mathbf{F}_{BB,j}^H \mathbf{F}_{RF}^H \right) = 1, \end{aligned} \tag{21}$$

where $\mathbf{V}_j$ is a constant weight matrix. Notice that, by setting

$$\mathbf{V}_j = \mathbf{M}_j^{-1}, \tag{22}$$

the Karush-Kuhn-Tucker (KKT) conditions of problems (20) and (21) can be satisfied simultaneously.

Proof. Taking the derivative of $-\sum_{j=1}^{K} I_{lb}(\mathbf{s}_j, \tilde{\mathbf{y}}_j)$ w.r.t $\mathbf{F}_{BB,k}$, we have

$$\frac{\partial\left(-\sum_{j=1}^{K} I_{lb}(\mathbf{s}_j, \tilde{\mathbf{y}}_j)\right)}{\partial \mathbf{F}_{BB,k}} = -\frac{\partial \sum_{j=1}^{K} \operatorname{tr}\left(\mathbf{M}_j \partial \mathbf{M}_j^{-1}\right)}{\partial \mathbf{F}_{BB,k}}, \tag{23}$$

where $\partial \log\det \mathbf{X} = \operatorname{tr}\left(\mathbf{X}^{-1}\partial\mathbf{X}\right)$ is utilized. Similarly, by taking the derivative of $\sum_{j=1}^{K} \operatorname{tr}(\mathbf{V}_j\mathbf{M}_j)$ w.r.t $\mathbf{F}_{BB,k}$, we have

$$\begin{aligned}\frac{\partial\left(\sum_{j=1}^{K} \operatorname{tr}(\mathbf{V}_j\mathbf{M}_j)\right)}{\partial \mathbf{F}_{BB,k}} &= \frac{\sum_{j=1}^{K} \operatorname{tr}\left(\partial\left(\left(\mathbf{M}_j^{-1}\right)^{-1}\right)\mathbf{V}_j\right)}{\partial \mathbf{F}_{BB,k}} \\ &\overset{(a)}{=} -\frac{\sum_{j=1}^{K} \operatorname{tr}\left(\mathbf{M}_j\partial\left(\mathbf{M}_j^{-1}\right)\mathbf{M}_j\mathbf{V}_j\right)}{\partial \mathbf{F}_{BB,k}},\end{aligned} \tag{24}$$

where $\partial\mathbf{X}^{-1} = -\mathbf{X}^{-1}\partial(\mathbf{X})\mathbf{X}^{-1}$ is utilized in (a). When $\mathbf{V}_j = \mathbf{M}_j^{-1}$, The equivalence of (23) and (24) can be obtained. Considering that the constraints in (20) and (21) are identical, we conclude that the KKT conditions of the two optimization problems can be satisfied simultaneously.

We propose an alternating algorithm to solve the WMMSE problem. By fixing $\mathbf{F}_{BB,h}$, $h \neq k$, the corresponding Lagrange function of solve $\mathbf{F}_{BB,k}$ can be written as follows

$$\begin{aligned}L_{\mathbf{F}_{BB,k}} = &\sum_{j=1}^{K} \operatorname{tr}(\mathbf{V}_j\mathbf{M}_j) + \\ &\lambda\left[\sum_{i=1}^{K} \operatorname{tr}\left(\mathbf{F}_{RF}\mathbf{F}_{BB,j}\mathbf{F}_{BB,j}^H\mathbf{F}_{RF}^H\right) - 1\right],\end{aligned} \tag{25}$$

where λ is the Lagrange multiplier. By setting the partial derivative of $L_{\mathbf{F}_{BB,k}}$ to zero. $\mathbf{F}_{BB,k}$ can be solved as

$$\begin{aligned}\mathbf{F}_{BB,k} = &\left\{\sum_{j=1}^{K}\left[\hat{\mathbf{H}}_j^H\mathbf{W}_{BB,j}\mathbf{V}_j\mathbf{W}_{BB,j}^H\hat{\mathbf{H}}_j + \sigma_e^2\operatorname{tr}\left(\mathbf{V}_j\right.\right.\right. \\ &\left.\left.\left.\cdot\mathbf{W}_{BB,j}^H\mathbf{\Sigma}_j\mathbf{\Sigma}_j^H\mathbf{W}_{BB,j}\right)\mathbf{\Psi}_j^H\mathbf{\Psi}_j\right] + \lambda\mathbf{F}_{RF}^H\mathbf{F}_{RF}\right\}^{-1} \\ &\cdot\hat{\mathbf{H}}_k^H\mathbf{W}_{BB,k}\mathbf{V}_k.\end{aligned} \tag{26}$$

Notice that, the optimum λ must be positive and the power constraint is a decreasing function of λ for $\lambda > 0$. Therefore, one-dimensional search techniques can be utilized to λ. We adopt the bisection method by setting the minimum Lagrange multiplier as $\lambda_{min} = 0$ and the maximum Lagrange multiplier as a pre-defined value λ_{max}. By substituting λ into (26), $\mathbf{F}_{BB,k}$ can be obtained. The steps of the proposed robust beamforming scheme for multi-user systems are summarized in Algorithm 1.

Algorithm 1. Proposed robust hybrid beamforming design

Require: Construct $\mathbf{F}_{BB}$ randomly; set λ_{min}, λ_{max}, and the termination criteria ϵ_1 and ϵ_2;

1: Calculate analog precoders $\mathbf{F}_{RF,k}$ for all k according to (3);
2: Calculate analog combiners $\mathbf{W}_{RF,k}^H$ for all k according to (4);
3: **repeat**
4:     Update digital combiners $\mathbf{W}_{BB,k}$ for all k according to (17);
5:     Update MMSE matrix $\mathbf{M}_k$ for all k according to (19);
6:     Update weighted matrix $\mathbf{V}_k = \mathbf{M}_k^{-1}$ for all k;
7:     **while** $\lambda_{max} - \lambda_{min} > \epsilon_1$ **do**
8:         setting $\lambda = \frac{\lambda_{max}+\lambda_{min}}{2}$;
9:         calculate $\mathbf{F}_{BB,k}$ for all k according to (26);
10:         **if** $\sum_{j=1}^{K} \mathrm{tr}\left(\mathbf{F}_{RF}\mathbf{F}_{BB,j}\mathbf{F}_{BB,j}^H\mathbf{F}_{RF}^H\right) < 1$ **then**
11:             $\lambda_{max} = \lambda$;
12:         **else**
13:             $\lambda_{min} = \lambda$;
14:         **end if**
15:     **end while**
16: **until** The change of $\sum_{j=1}^{K} \mathrm{tr}\left(\mathbf{V}_j\mathbf{M}_j\right)$ is below ϵ_2.

Since the constant weighted matrix $\mathbf{V}_k$ is updated with each iteration, it does not ensure that the objective function decreases monotonously. We are unable to directly demonstrate the convergence of the proposed algorithm. Fortunately, its convergence can be proved by proving the convergence of an equivalent optimization problem as follows

$$\begin{aligned} \min_{\{\mathbf{F}_{BB,j},\mathbf{V}_j\}} \quad & \sum_{j=1}^{K} \left[\mathrm{tr}\left(\mathbf{V}_j\mathbf{M}_j\right) - \log\det \mathbf{V}_j\right] \\ \text{s.t.} \quad & \sum_{j=1}^{K} \mathrm{tr}\left(\mathbf{F}_{RF}\mathbf{F}_{BB,j}\mathbf{F}_{BB,j}^H\mathbf{F}_{RF}^H\right) = 1. \end{aligned} \tag{27}$$

When $\mathbf{F}_{BB,j}$ and $\mathbf{V}_j$ are fixed, optimizing (27) w.r.t $\mathbf{W}_{BB,j}$ gives the same result as step 5 in Algorithm 1. Similarly, by fixed other variables, optimizing (27) w.r.t $\mathbf{V}_j$ and $\mathbf{F}_{BB,j}$ gives the same results as steps 6 and 9 in Algorithm 1, respectively. Thus, the objective function in (27) decreases monotonically. A similar procedure was adopted in [16] to prove the monotonous convergence of equivalent problems, in which traditional fully digital transceivers are optimized iteratively under perfect CSI assumptions. According to [16], the objective function in (27) has a lower bound, so the convergence of Algorithm 1 to a local minimum can be guaranteed.

4 Simulation Results

In this section, the sum rate and energy efficiency of the proposed beamforming scheme are evaluated for different configurations. The number of users is

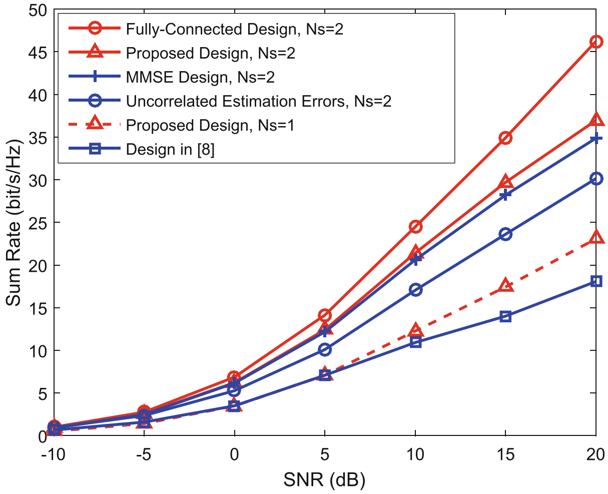

Fig. 2. Sum rate comparison at different SNR.

$K = 4$. The propagation paths for different channels are all set as $N_p = 4$. The elements of mmWave channels, i.e., complex gains of propagation paths, and AWGN matrices obey complex Gaussian distribution. The AoAs and AoDs follow Laplacian distribution with uniformly distributed mean angles over $[-\frac{\pi}{2}, \frac{\pi}{2}]$. The angular spread is restricted to $10°$. The variances of estimation errors for different channels are assumed to be identical for simplicity. The signal-to-noise ratio (SNR) is defined as $10\lg\frac{1}{\sigma_n^2}$. The stopping criteria in Algorithm 1 are set as $\epsilon_1 = 10^{-8}$, $\epsilon_2 = 10^{-4}$. λ_{min} and λ_{max} are set to 0 and 50, respectively. All simulations are averaged over 1000 channel realizations.

Figure 2 shows the sum rate comparison between the proposed design and other existing designs. The fully-connected structure design is obtained by replacing sub-connected structures in the proposed design with fully-connected structures. The MMSE design minimize MSE by replacing the weighted matrix with an identity matrix. The design based on uncorrelated estimation errors is obtained by forcing the covariance matrices to be identity matrices in the proposed design. The antenna configurations are set as $N = 64$, $M = 8$, $\sigma_e^2 = 0.5$, $N_s = N_{rf}$. As we can see, the proposed design is only inferior to the fully-connected design. The proposed design outperforms the MMSE design by 5.28% at SNR = 15 dB. The performance gap caused by model mismatch is quite large. The proposed design outperforms the design based on uncorrelated estimation errors by 25.6% at SNR = 10 dB. Besides, the performance of the non-robust joint design with sub-connected structures in [8], which only applies to single data stream users is also illustrated in the figure. We can see the performance improvement is significant as the number of data streams increases. When the number of data streams reduced to one, the proposed design still outperforms the design in [8] by 27.6% .

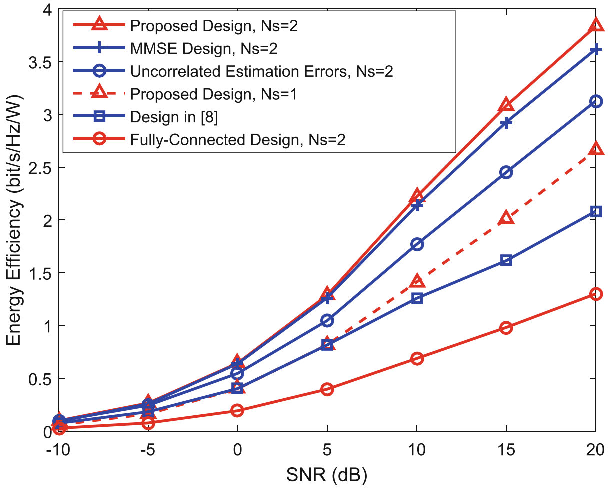

Fig. 3. Energy efficiency at different SNR.

Figure 3 shows the energy efficiency comparison of the designs in Fig. 2. The power consumption at the BS side can be expressed as [2]

$$\begin{aligned} P_{fully} =& N(KN_{rf}+1)P_{PA} + NKN_{rf}P_{PS} + P_{BB} + KN_{rf} \\ & \cdot (P_{RFC} + P_{DAC}), \\ P_{sub} =& NP_{PA} + NP_{PS} + P_{BB} + KN_{rf}(P_{RFC} + P_{DAC}), \end{aligned}$$

where P_{PA} denotes the power of power phase amplifiers; P_{PS} denotes the power of phase shifters. P_{BB} denotes the power of baseband processing; P_{RFC} denotes the power of RF chains; P_{DAC} denotes the power of digital-to-analog converts. The power consumption at the user side can be obtained by corresponding substitutions. The value of each component follows [2]. As we can see, although the fully-connected design provides higher sum rate, its energy efficiency is the worst. The sub-connected designs provide better energy efficiency due to the reduced number of phase shifters. The proposed design outperforms the fully-connected design by 226% at SNR = 15 dB. Besides, the proposed design has the best energy efficiency and outperforms the MMSE design and the design based on uncorrelated estimation errors by 5.3% and 25.7% respectively at SNR = 15 dB. Furthermore, with the increase of the number of data streams, the system has higher energy efficiency. Even if the number of data streams is reduced to one, the proposed design outperforms the design in [8] by 24.4% at SNR = 15 dB.

5 Conclusion

Correlated estimation errors and sub-connected structures are considered to design a robust beamforming scheme for MU mmWave systems in this paper. A two-stage design procedure is proposed. In the first stage, analog beamformers are designed to maximize channel gains. In the second stage, digital beamformers are designed to maximize mutual information and handle inter-user interference. The simulation results confirm the superiority of the proposed design in comparison with other existing designs.

References

1. Heath, R.W., Gonzalez-Prelcic, N., Rangan, S., Roh, W., Sayeed, A.M.: An overview of signal processing techniques for millimeter wave mimo systems. IEEE J. Sel. Topics Signal Process. **10**(3), 436–453 (2016)
2. Mendez-Rial, R., Rusu, C., Gonzalez-Prelcic, N., Alkhateeb, A., Heath, R.W.: Hybrid mimo architectures for millimeter wave communications: Phase shifters or switches? IEEE Access **4**, 247–267 (2016)
3. Kim, M., Lee, Y.H.: Mse-based hybrid rf/baseband processing for millimeter-wave communication systems in mimo interference channels. IEEE Trans. Veh. Technol. **64**(6), 2714–2720 (2015)
4. Nguyen, D.H.N., Le, L.B., Le-Ngoc, T., Heath, R.W.: Hybrid mmse precoding and combining designs for mmwave multiuser systems. IEEE Access **5**, 19167–19181 (2017)
5. Wu, X., Liu, D., Yin, F.: Hybrid beamforming for multi-user massive mimo systems. IEEE Trans. Commun. **66**(9), 3879–3891 (2018)
6. Ha, V.N., Nguyen, D.H.N., Frigon, J.F.: System energy-efficient hybrid beamforming for mmwave multi-user systems. IEEE Trans. Green Commun. Netw. **4**(4), 1010–1023 (2020)
7. Zhang, Y., Du, J., Chen, Y., Li, X., Rabie, K.M., Kharel, R.: Near-optimal design for hybrid beamforming in mmwave massive multi-user mimo systems. IEEE Access **8**, 129153–129168 (2020)
8. Li, A., Masouros, C.: Hybrid analog-digital millimeter-wave mu-mimo transmission with virtual path selection. IEEE Commun. Lett. **21**(2), 438–441 (2017)
9. Garcia-Rodriguez, A., Venkateswaran, V., Rulikowski, P., Masouros, C.: Hybrid analog-digital precoding revisited under realistic rf modeling. IEEE Wireless Commun. Lett. **5**(5), 528–531 (2016)
10. Zhao, L., Ng, D.W.K., Yuan, J.: Multi-user precoding and channel estimation for hybrid millimeter wave systems. IEEE J. Sel. Areas Commun. **35**(7), 1576–1590 (2017)
11. Jiang, L., Jafarkhani, H.: Multi-user analog beamforming in millimeter wave mimo systems based on path angle information. IEEE Trans. Wireless. Commun. **18**(1), 608–619 (2019)
12. Zheng, L., Liu, D., Wen, Z., Zou, J.: Robust beamforming for multi-user miso full-duplex swipt system under non-linear energy harvesting model. IEEE Access **9**, 14387–14397 (2021)
13. Luo, Z., Zhao, L., Liu, H., Li, Y.: Robust hybrid beamforming in millimeter wave systems with closed-form least-square solutions. IEEE Wireless Commun. Lett. **10**(1), 156–160 (2021)
14. Zhang, R., Leung, S.H., Luo, Z., Wang, H.: Precoding design for correlated mimo-af relay networks with statistical channel state information. IEEE Trans. Signal Process. **66**(22), 5902–5916 (2018)

15. Xing, C., Ma, S., Fei, Z., Wu, Y.C., Poor, H.V.: A general robust linear transceiver design for multi-hop amplifyand-forward mimo relaying systems. IEEE Trans. Signal Process. **61**(5), 1196–1209 (2013)
16. Christensen, S.S., Agarwal, R., De Carvalho, E., Cioffi, J.M.: Weighted sum-rate maximization using weighted mmse for mimo-bc beamforming design. IEEE Trans. Wireless Commun. **7**(12), 4792–4799 (2008)